Supporting Information for "Prebiotically relevant mixed fatty acid vesicles support anionic solute encapsulation and photochemically catalyzed transmembrane charge transport"

Jonathan L. Cape, Pierre-Alain Monnard and James M. Boncella.

Contents:

I. Micrographic analysis of solute encapsulated vesicles.

In this work we have used a combination of chromatographic analyses and time dependent solute leakage to characterize the permeability of charged solutes to fatty acid vesicles. These analyses alone do not provide conclusive proof of solute encapsulation. Here we provide a micrographic analysis of the solute encapsulated vesicle preparation and a chromatographic analysis of solute binding to the outside of pre-prepared vesicles to demonstrate two essential features of the encapsulated preparation: 1) That the internal, and not external, volume of this vesicle preparation contains solute dye, and 2) that passage of the dye through the size exclusion resin with the high molecular weight fraction is not due to adsorption to the outside of the vesicles.

Microscopic analysis of pyranine-encapsulated vesicles (1000 X) shows a field of small fluorophore-filled spheres, the vesicles, on a black background. Their glow is due to encapsulated pyranine dye. No fluorescence is observed in the buffer surrounding the vesicles. Shown below are selected micrographs of narrow field views (1000X power with an additional 4X magnifying lense placed in front of the camera aperture). These images show discrete glowing vesicles (albeit blurry due to Brownian movement and the limited resolution of our microscopic system). The fact that these images show a near even distribution

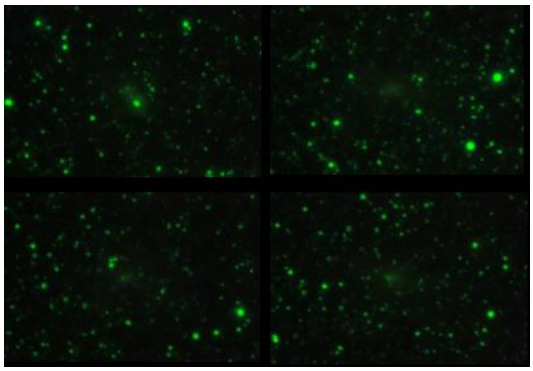

Figure 1. Narrow field views (1000X oil immersion) of pyranine encapsulated vesicles made from 30 mM decanoic acid, 50 mM phosphate, pH 7.25. Vesicles were prepared in the presence of 2.27 mM pyranine dye for encapsulation, then purified by size exclusion chromatography on a sephadex G-25 resin as described in the text. The glow in each of the vesicles is due to fluorescence of the pyranine dye. We observed extensive photobleaching of this dye, likely due to photo-oxidation under the intense illumination field. This issue required fast shutter speeds and high ISO settings, limiting the resolution of these micrographs; only selected images showing relatively stationary vesicles are shown.

of fluorescence throughout the vesicles, and not a concentration of fluorescence intensity around the vesicle edges, further supports the notion that the solutes are encapsulated and not bound to the membrane. Similar results were also obtained for encapsulation of the anionic ruthenium based dye, Tris-(5,5'-dicarboxy-2,2'-bipyridine)ruthenium(III) dichloride (Figure 2).

As a further test for the possibility of membrane binding, we prepared vesicles in phosphate buffer then added pyranine to the sample. Assuming these vesicles stay intact, and that the passage of pyranine across the membranes is slow (as suggested by the experiments described in the text), the added pyranine should stay confined to the outer aqueous domain. If the solute binds to the outside of the membranes one should observe a high molecular weight fraction elute followed by a low molecular weight fraction, similar to those chromatograms shown in Figure 3 of the text. However, if the solute does not bind to the outer surface, one should only observe a low molecular weight fraction elute on longer timescales.

The size exclusion chromatogram run for this experiment is shown in Figure 3 below, compared with the initial size exclusion run to initially separate the encapsulated fraction from free solute. This data demonstrates that the dye pyranine does not bind to the outer membrane surface.

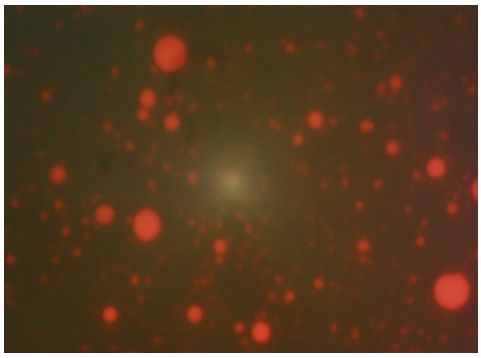

Figure 2. Fluorescence micrograph of the anionic dye $Ru(dcb)_3^{4-}$ encapsulated inside decanoic acid vesicles 4 hours post-preparation.

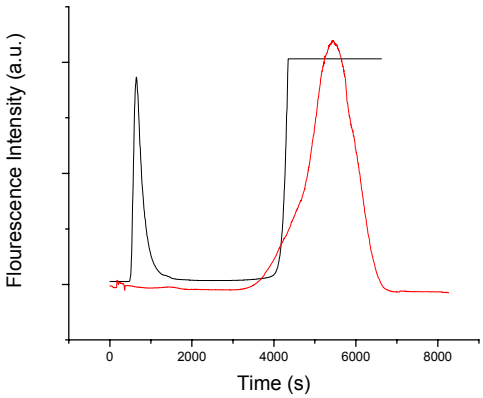

Figure 3. Size exclusion chromatography of the initial encapsulation (black), and test for binding of pyranine to the outer surface of preformed vesicles (red).

II. DLS-measured hydrodynamic radii and polydispersity indices.

Table 1. Size and polydispersity indices of complex fatty acid mixture SUV's.

Fatty Acid Mixture	R_m (nm)	P
C10-C2	86	3.71
C10-C3	79	1.16
C10-C4	109	1.15
C10-C5	104	1.11
C10-C6	103	1.23
C10-C7	94	1.13
C10-C8	106	1.21
C10-C9	56	5.82
C10	92	1.53

III. Estimate of the number of PAH species solublized per vesicle.

The measured hydrodynamic radii of ~100 nm serves as an approximate estimate of the vesicle diameter, and the measured values of ~20 Å^2 for the lipid headgroup area [1] and 28 Å for bilayer thickness of decanoic acid [2] allow an estimate of the inner and outer surface areas, as well as the number of FA molecules residing in the inner and outter leaflets per vesicle.

$S_{inner} = 1.19 \times 10^7$ angstroms^2 $\qquad$ FA in inner leaflet $= 5.94 \times 10^5$

$S_{outer} = 1.27 \times 10^7$ angstroms^2 $\qquad$ FA in outter leaflet $= 6.28 \times 10^5$

$$\text{Total FA / vesicle} = 1.22 \times 10^6$$

In our experiments we use solutions that are 50 mM in total fatty acids at pH 7.2. The CVC at this pH is approximately 20 mM. Thus, each solution must contain approximately 20 mM soluble fatty acids (and sodium salts), with the remainder going to form vesicle species. Per mL, we can estimate the number of fatty acid molecules forming vesicle species as

$$[([FA] - CVC)*0.001]*N = 1.80 \times 10^{19} \text{ molecules forming vesicles per mL}$$

Dividing this value by the total number of lipid molecules in each vesicle, dividing by *N* (Avagadro's number), then converting mL to liters yields the apparent molarity of vesicles.

$$[(\text{Molecules FA in vesicles mL}^{-1} / \text{molecules per vesicle}) / N]*1000 \text{ (mL/L)} = 2.45 \times 10^{-8} \text{ M FA vesicles}$$

From this concentration we can estimate the approximate number of PAH molecules per vesicle that were solublized in our preparations (starting from crystalline Perylene or 2,3a-naphthopyrene).

$$201 \text{ nM Perylene} / 24.5 \text{ nM vesicles} = 8.2 \text{ per vesicle}$$

$$342 \text{ nM 2,3a-naphthopyrene} / 24.5 \text{ nM vesicles} = 13.9 \text{ per vesicle}$$

These values are considered upper limits, thus we consider the actual solublilty to range between 1-10 per vesicle as given in the text.

IV. Thermodynamic analysis of photoinduced electron transfer reactions.

Electrochemical data are incomplete for one of the PAH species invesitigated in this work, naphtho[2,3a]pyrene. Data for perylene however are available and allow an estimate of the excited state reduction potentials for both oxidative and reductive quenching pathways.

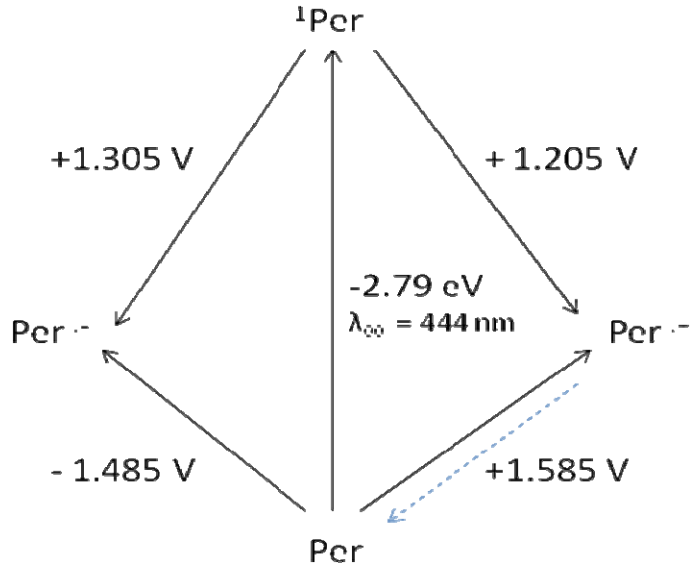

$E_{1/2}$ (EDTA / EDTA$^{\cdot}$) = ~1.5 V for initial one-electron oxidation (estimate from Hoffman 1988)

$E_{1/2}$ ($FeCN_6^{3-}$ / $FeCN_6^{4-}$) = 0.375 V

Reactions:

^{1}Per + EDTA → Per$^{\cdot-}$ + EDTA$^{\cdot}_{ox}$ ΔE = -0.195 V

^{1}Per + $Fe(CN)_6^{3-}$ → Per$^{\cdot+}$ + $Fe(CN)_6^{4-}$ ΔE = 0.83 V

Per$^{\cdot-}$ + $Fe(CN)_6^{3-}$ → Per + $Fe(CN)_6^{4-}$ ΔE = 1.86 V

Per$^{\cdot+}$ + EDTA → Per + EDTA$^{\cdot}_{ox}$ ΔE = 0.085 V

Cumulative potentials for either pathway:

Anion radical intermediate: ΔE = 1.665 V

Cation radical intermediate: ΔE = 0.915 V

V. X-ray diffraction of decanoic acid / sodium decanoate films containing PAH species.

We investigated thin film X-ray diffraction from partially hydrated decanoic acid/decanoate multilayers to provide a first order estimate of any perturbations that might occur on inclusion of the PAH species perylene and naphtho(2,3a)pyrene into vesicles bilayers. Although such films are a different physical phase than the soluble vesicles investigated in this work, these measurements provide valuble information regarding the estimated bilary thickness which cannot be obtained easily for solublized vesicles.

Films were prepared by layering 50-100 μL of a 50 mM decanoic acid / sodium decanoate vesicle suspension (50 mM phosphate, pH 7.2) onto a coarse glass substrate. Wet films were allowed to dry for 2 hours prior to analysis. The degree of dryness did not greatly affect the measurements, consistent with diffraction from the bilayer spacing, and not inter-lamellar spacings.

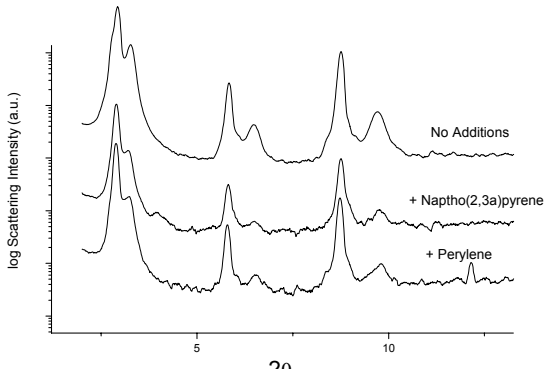

Figure 4. X-ray diffraction of thin films of decanoic acid / sodium decanoate with added PAH's. The vertical axis is in log scale for clarity.

Figure 4 shows diffraction data from decanoic acid / sodium decanoate films containing both perylene and naphtho(2,3a)pyrene in ten-fold excess of the kinetics experiments described in the text. Literature examples [3,4] of fatty acid / sodium salt films show similar scattering profiles to those presented in Figure 4. Three orders of diffraction are observed for two liquid crystalline forms, the so called 'B' and 'C' forms descrbed in detail by Francis[4] and Fieldes[3]. The two liquid crystalline forms presumably differ in the tilt angle of the bilayer normal with respect to the substrate. Thus, these measurements do not directly yield the bilayer thickess, but instead yield d-spacings corresponding to $D\cos(\theta)$, where D is the bilayer spacing, $\theta = 90 - \varphi$, where φ is the tilt angle of the membrane normal with respect to the substrate normal. The d-spacings obtained for these films are 28.1 and 24.7 angstroms for B and C forms, respectively. No gross changes to the relative intesities or peak widths are observed on addition of perylene and naphtho(2,3a)pyrene.

Supporting Information References.

(1) Datta, A.; Kmetko, J.; Richter, A. G.; Yu, C. J.; Dutta, P.; Chung, K. S.; Bai, J. M. *Langmuir* **1999**, *16*, 1239-1242.

(2) Bond, A. *New Journal of Chemistry* **2004**, *28*, 104-114.

(3) Fieldes, M.; Hartman, L. *Proceedings of the Royal Society of London. Series A, Mathematical and Physical Sciences* **1955**, *233*, 195-202.

(4) Francis, F.; Piper, S. H.; Malkin, T. *Proceedings of the Royal Society of London. Series A, Containing Papers of a Mathematical and Physical Character* **1930**, *128*, 214-252.